Journal of Power Sources 241 (2013) 449–453

Contents lists available at SciVerse ScienceDirect

Journal of Power Sources

journal homepage: www.elsevier.com/locate/jpowsour

Short communication

A single flow zinc//polyaniline suspension rechargeable battery

Yongfu Zhao, Shihui Si*, Cui Liao

College of Chemistry and Chemical Engineering, Central South University, Changsha 410083, PR China

HIGHLIGHTS

- The energy-dense PANI suspensions were obtained using the compact PANI materials.
- PANI suspension as flowing cathode was used for the design of flow battery.
- Use of microporous membrane enabled anolyte and cathodic materials to renew.

ARTICLE INFO

Article history:
Received 1 February 2013
Received in revised form
30 March 2013
Accepted 19 April 2013
Available online 30 April 2013

Keywords:
Polyaniline suspension
Single flow battery
Zinc
Flowing cathode

ABSTRACT

Both the electrochemical activity and the energy density of polyaniline (PANI) microparticles suspensions are enhanced by using the compact PANI powder, which is synthesized galvanostatically with 4,4′-diaminobiphenyl as additive. A Zn//PANI suspension rechargeable flow battery system is proposed, in which the flowable PANI suspension is used as cathode electroactive material, zinc plate as anode. A microporous membrane is used as separator to prevent PANI particles from getting into the anode compartment. Results obtained from the small laboratory battery show that the discharge capacity density gradually decreases with number of cycles and the average of discharge capacity loss during 32 cycles is about 0.07% per cycle. However, an average coulombic efficiency of 97% has been achieved at the current density of 20 mA cm^{-2} and the value of coulombic efficiency shows no significant change during 32 charge/discharge cycles. The flow-through mode for PANI cathode material enables the PANI-based battery to operate at a higher current density in comparison with the conventional Zn–PANI film batteries, and the present findings can mark a new route to improve the performance of conductive polymer-based energy storage devices.

1. Introduction

Polyaniline (PANI) has attracted considerable attention due to its high conductivity, low cost, good redox reversibility and environmental stability. These features make it an interesting candidate for electrode materials in rechargeable electrical energy storage devices, including supercapacitors [1,2] and rechargeable batteries [3–8]. Among the family of PANI-base batteries, a considerable interest has been shown in aqueous PANI-base batteries, typically, aqueous Zn–PANI batteries composed of PANI cathode and zinc anode with aqueous electrolyte. In comparison with classical batteries and aprotonic cells, these batteries exhibit a lot of advantages such as: ecological acceptability, low cost and easy manufacture (due to uses of water based electrolytes).

Up to now Zn–PANI batteries have not been commercialized for some reasons. First of all, in PANI film batteries, only the outer layer of PANI films can contribute to the charge/discharge processes, resulting in the decay of the specific capacity. Then, the higher current densities of charge/discharge lead to a remarkable decrease in the coulombic efficiency of the batteries [7–9]. Unlike conventional rechargeable batteries storing the electrical energy within solid electrode materials, the redox flow batteries (RFBs) store the electrical energy in the external reservoirs, as the most promising large scale energy storage systems, including Fe/Cr [10], V [11], polysulfide/Br_2 [12], Fe/V [13]. Despite its technological and commercial advances made in recent years, no existing RFB is commercially ready for the final market entry owing to the challenges they are facing. These systems require the employment of ion exchange membranes, which increases the complexity and brings about a net volumetric transfer of water. Regarding materials, expensive vanadium resources and Nafion-based membranes are the two factors that inflate the capital

* Corresponding author. Tel.: +86 731 88876490; fax: +86 731 88879616.
E-mail address: sishihui@mail.csu.edu.cn (S. Si).

0378-7753/$ – see front matter © 2013 Elsevier B.V. All rights reserved.
http://dx.doi.org/10.1016/j.jpowsour.2013.04.095

cost of all-vanadium RFBs. In addition, traditional sulfuric-acid-based all-vanadium RFB is significantly hindered by the vanadium ion solubility and stability in electrolyte solutions, which limit the system not only to a low energy density but also to a narrow operational temperature. Besides technical difficulties, pollution is always accompanied with the all-vanadium RFB. Recently, a semi-solid Lithium rechargeable flow battery was proposed, in which the inherent advantages of flow architecture were retained while dramatically increasing energy density by using suspensions of energy-dense active materials [14]. However, the discharging current density of the system was by far lower than that of conventional RFB.

In this study, PANI materials were prepared using the chemical and electrochemical synthesis methods, and characterized by scanning electron microscope and FT-IR spectrum. The electrochemical properties of PANI particles suspensions were investigated with cyclic voltammetry, potentiostatic discharge. Herein, we present a new strategy for Zn//PANI batteries using PANI suspension in a flow-through mode as cathode, zinc plate as anode. Transition from solid film to a flow-through mode for PANI cathode enables Zn–PANI suspension rechargeable flow battery (Zn–PANI–FB) to circumvent the issues that conventional Zn–PANI batteries and RFBs existed.

2. Experimental section

PANI powder was synthesized galvanostatically on the graphite plate in a solution containing 0.5 M aniline and 1.0 M $HClO_4$ with 25 mM 4,4′-diaminobiphenyl as additive. Prior to experiments, the graphite electrodes were mechanically polished and cleaned in an ultrasonic bath in water/ethanol mixture. The PANI was collected by scratching with a plastic knife, and then washed with dilute $HClO_4$ and deionized water. Finally, the obtained PANI powder was subjected to grinding using cutting mill for the preparation of micro-sized PANI particles.

The chemical polymerization of PANI was carried out as following: 0.02 mol of purified aniline was dissolved in 50 mL of 1.0 M $HClO_4$ aqueous solution, then 0.02 mol of $(NH_4)_2S_2O_8$ was slowly added into the aniline solution and stirred for 10 h at ambient temperature. The precipitated green PANI salt was filtered, and washed with dilute $HClO_4$ and deionized water until the washing liquid was colorless.

PANI suspensions were prepared by dispersing above PANI powder into a solution of 2.0 M $ZnCl_2$ and 2.0 M NH_4Cl. In the present experiment, pH of electrolyte solution was adjusted to 4.5 with HCl or ammonia hydroxide, and no other buffer was used except NH_4Cl.

PANI film was electrochemically grown onto gold electrode by cyclic voltammetry between −0.2 V and 0.8 V at scanning rate of 50 mV s^{-1} in 1.0 M $HClO_4$ and 0.2 M aniline solution. After approximately 50 cycles, the electrodeposited PANI film was rinsed with dilute $HClO_4$ and deionized water.

All electrochemical experiments were carried out with CHI420 electrochemical analyzer (ChenHua Instrument Co., China). The PANI-modified gold electrode or a bare gold electrode with diameter of 2 mm was used as the working electrode, and a platinum wire as counter electrode, and all potentials were referred to saturated calomel electrode (SCE). The potentiostatic discharge of PANI suspension was carried out at −0.3 V by using a bare gold electrode in the stirred PANI suspension. The galvanostatic charge/discharge measurements of PANI and zinc electrodes were performed in a three-electrode system. All charge/discharge experiments on Zn–PANI suspension flow battery were conducted with an eight-channel BTS battery test system (Newware Ltd., China).

Viscosity measurement of suspensions was carried out in the range of shear rates 1–100 s^{-1} at 25 °C using a concentric cylinder viscometer (Haake VT550, Germany). Scanning electron microscopy (SEM) was performed on a JEOL JSM-6360F scanning electron microscope. FT-IR spectrum of the electropolymerized PANI was recorded with a Nicolet 380 FT-IR spectrophotometer.

3. Results and discussion

3.1. Electrochemical behaviors of PANI materials in solution of $ZnCl_2$ and NH_4Cl

As shown in Fig. 1, the cyclic voltammograms of PANI microparticles suspended in solution containing 2.0 M $ZnCl_2$ and 2.0 M NH_4Cl with pH 4.5 exhibit a pair of well-defined redox peaks at 0.27 V and 0.02 V, whereas PANI film shows two oxidation peaks at 0.22 V, 0.48 V and a reduction peak at 0.13 V (inset in Fig. 1). The anodic peak for PANI film at 0.48 V may be due to the oxidation of aniline oligomer incorporated into PANI matrix. The couple of peaks at the potential of 0.27 V and 0.02 V of PANI microparticles suspensions corresponding to the redox peaks at 0.22 V and 0.13 V of PANI film are attributed to the doping/dedoping of Cl^- anions to/from PANI, and the cyclic voltammograms of PANI suspensions are almost similar to that of PANI film [15]. The negative shift of cathodic peak in the case of electropolymerized PANI microparticles is probably due to the presence of charge transfer resistance between the PANI particles and the gold electrode. From CV curve 1 and 2 in Fig. 1, it can be seen that the peak current of electropolymerized PANI microparticles suspension is significantly higher than that of chemically synthesized PANI suspension, which means the higher redox switching rate for the electropolymerized PANI microparticles in comparison with the chemically synthesized PANI microparticles. Moreover, the experimental results for the potentiostatic test are shown in Fig. 2. The current of the electropolymerized PANI microparticles with additive of 4,4′-diaminobiphenyl (~0.35 mA) is nearly ten times higher than that of PANI chemically synthesized (~0.037 mA), suggesting that the electrochemical activity is enhanced for the PANI microparticles electrochemically synthesized with additive of 4,4′-diaminobiphenyl.

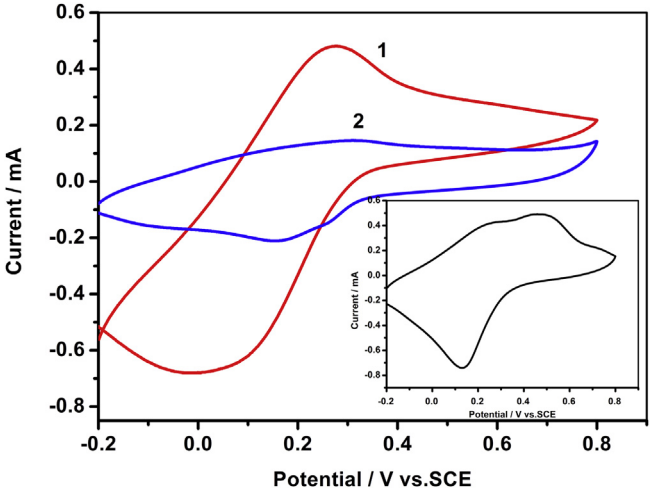

Fig. 1. Cyclic voltammograms of PANI suspensions with particles content of 50 g L^{-1} (W/V): (1) electrochemical synthesis (average particle size about 12.5 μm), (2) chemical synthesis (average particle size about 14.1 μm). PANI film (the inset) in solution containing 2.0 M $ZnCl_2$, 2.0 M NH_4Cl with pH at 4.5. Working electrode: gold electrode with diameter of 2 mm. Scan rate: 50 mV s^{-1}.

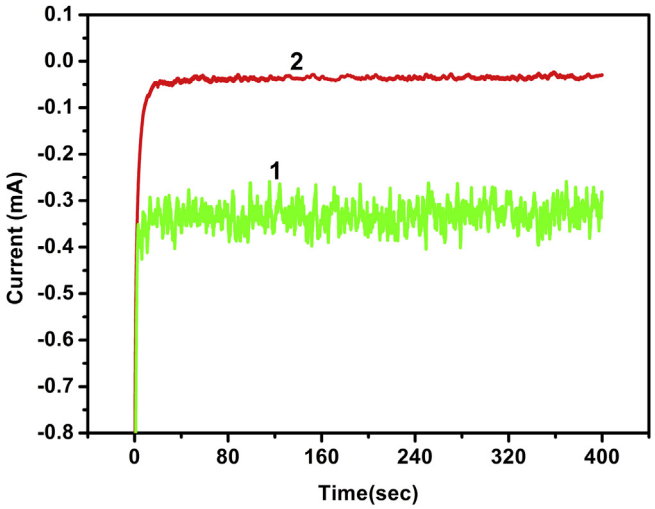

Fig. 2. Potentiostatic test of PANI suspensions (50 g L^{-1}): (1) electrochemical synthesis (average particle size about 12.5 μm), (2) chemical synthesis (average particle size about 14.1 μm). Working electrode: gold electrode with diameter of 2 mm; the discharge potential: −0.3 V; in stirred condition.

3.2. Characterization of PANI cathode material

Fig. 3 shows the FT-IR spectrum for the electropolymerized PANI. The bands at 1487 and 1563 cm^{-1} are assigned to C═C stretching of the benzenoid and quinoid rings, respectively. The peak at 1293 cm^{-1} is assigned to C–N stretching of secondary amine of PANI backbone, and the band at 1239 cm^{-1} corresponding to the C–N stretching vibration is the characteristic of the conducting PANI emeraldine salt form. The bands at 1129 cm^{-1} and 796 cm^{-1} can be assigned to an in plane bending vibration of C–H (mode of N═Q═N, Q = NH^{+}–B, and B–NH^{+}–B) and the C–H out-of-plane deformation vibration of the benzenoid group, respectively. Hence, the main form of PANI cathode material is doped PANI emeraldine salt [16].

The SEM micrographs of above PANI particles are shown in Fig. 4. The sponge-like structure for the chemically synthesized PANI and a compact, scaly morphology for the electropolymerized PANI are observed. The scaly structure of the electropolymerized

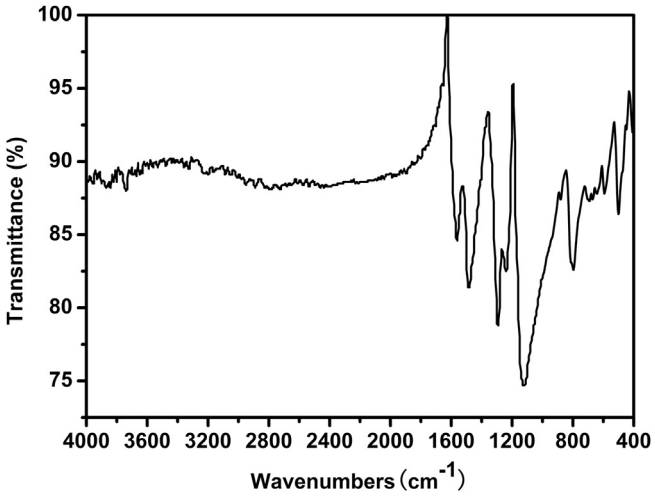

Fig. 3. SEM images of the surfaces of PANI powder: (a) chemical synthesis, (b) electrochemical synthesis.

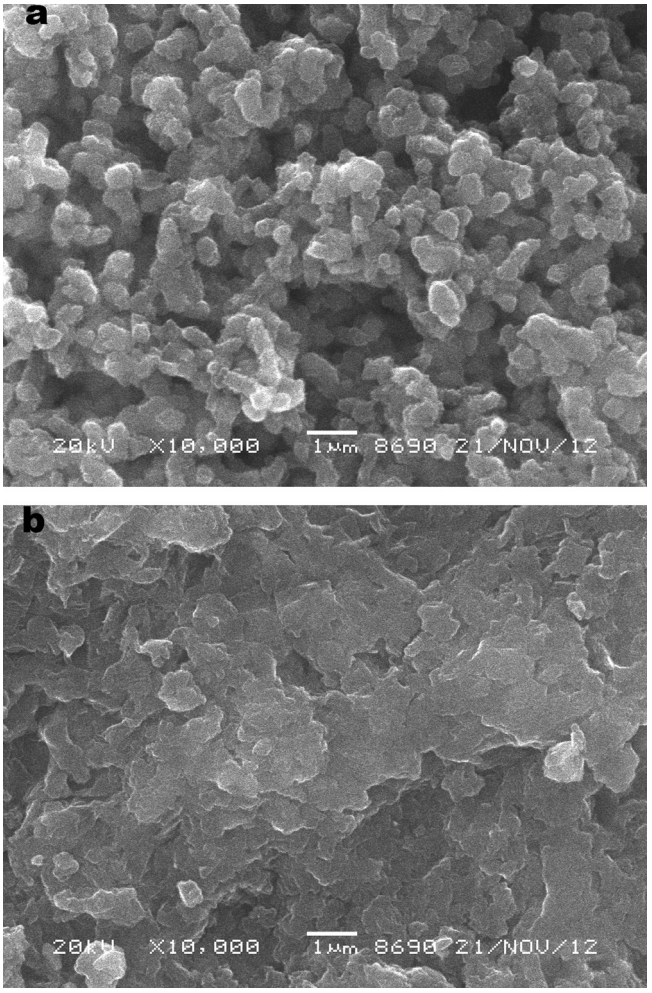

Fig. 4. FT-IR spectra of the electropolymerized PANI.

PANI is favorable for contact among PANI particles, which is essential for achieving a high ionic conductivity. The bulk density of PANI powder synthesized galvanostatically with additive of 4,4′-diaminobiphenyl was estimated about 0.97 g cm^{-3}, and a flowable suspension with content of 420 g L^{-1} was achieved by using the present electropolymerized PANI, whereas the upper limit content for the chemically synthesized PANI (~0.35 g cm^{-3}) was about 150 g L^{-1} in the flowable suspension. In the following experiments, the electropolymerized PANI microparticles dispersed in the solution of $ZnCl_2$ and NH_4Cl were used as cathode material for the zinc PANI flow battery system.

3.3. Rheological behavior of PANI suspensions

The rheological behavior of PANI suspension, which is susceptible to its viscosity, is the concern for the design of flow battery. The shear viscosity of PANI suspensions was measured at various shear rates (shown in Fig. 5). It is observed that low content PANI suspensions (100, 200 g L^{-1}) exhibit initially shear-thinning (1–65 s^{-1}), reaching a minimum viscosity at a critical value of shear rate and then exhibit a shear-thickening behavior above the shear rates of 65 s^{-1}. And the shear thinning occurs for the PANI suspension of 300 g L^{-1} over the whole range of shear rates. The observed shear-thinning behavior may be attributed to the rupture of the aggregation and interlink between PANI particles resulting

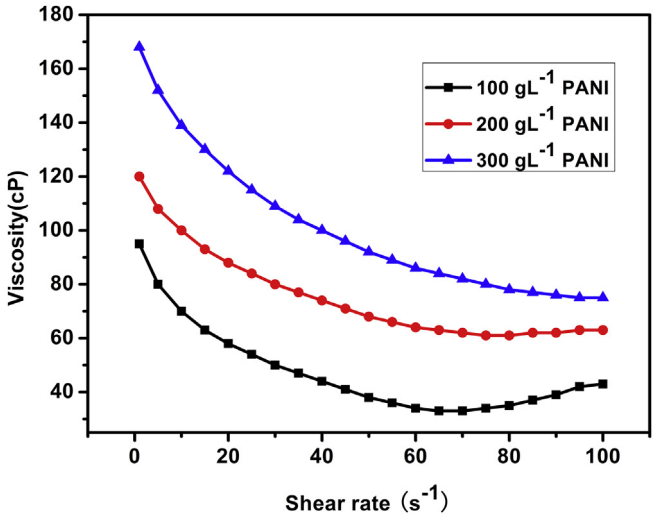

Fig. 5. Steady shear viscosity for PANI suspensions with various particles content (100, 200, 300 g L^{-1}).

from steady shear. The viscosities of the PANI suspensions are much higher than that of the 2.0 M V (V) solutions used in all-vanadium RFB, in which two pumps are used and the pumping dissipation/total-discharge-power ratio is about 2–3% [17,18]. However, the viscosities of PANI suspensions are ~10 times lower than that of the semi-solid active materials used in SSFC with two pumps, and the ratio of pumping dissipation to total-discharge-power is about 22% [14]. By comparison, in the present single flow system, it can be expected that the ratio will be less than 5%.

3.4. Schematic illustration and working mechanism of Zn–PANI–FB

The schematic illustration of Zn–PANI–FB is shown in Fig. 6. The battery system consists of an energy storage unit (a single pump and reservoir) and an energy conversion unit (a cell). The smooth graphite plate (4 cm^2 area) is used as cathode current-collector and flowing PANI suspension as cathode electroactive material, zinc plate (4 cm^2 area) as anode. A polypropylene microporous membrane (with a mean pore size of 0.5 μm, thickness of 0.18 mm and active area of 4 cm × 1 cm) is used as separator to prevent PANI particles from getting into the anode compartment, differing from the conventional RFBs with the use of the ion-exchange membrane as a separator. Application of microporous membrane remarkably simplifies the configuration of cell and reduces the cost of the battery significantly due to the elimination of the problems associated with an ion-exchange membrane. The present system works in a mode different from the conventional RFB. During the battery working process, the PANI suspension is pumped into the cathode compartment, where part of $ZnCl_2$ and NH_4Cl solution penetrates into the anode compartment via the microporous membrane, the remained fluid containing PANI particles flows through the cathode compartment, and the regeneration of the anodic and cathodic active material can be achieved simultaneously in the single fluid system.

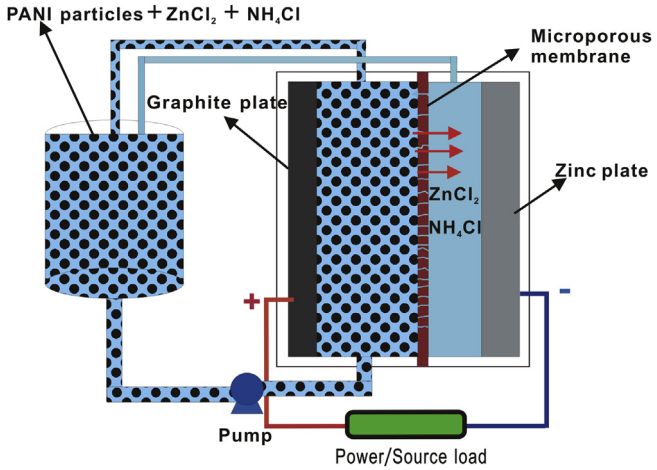

Fig. 6. Schematic illustration of the Zn–PANI–FB.

During the process of charge, Zn^{2+} cations are deposited on zinc plate from the electrolytic solution and PANI particles in the opposite compartment are oxidized with Cl^- incorporation. On the contrary, while discharging, metallic zinc is dissolved into the electrolytic solution and the PANI particles are reduced with Cl^- dedoping. Therefore, the overall reaction of battery is shown in Equation (1):

$$n\mathrm{Zn} + \mathrm{PANI}^{+}\left(\mathrm{Cl}^{-}\right)_{2n} \underset{\text{charge}}{\overset{\text{discharge}}{\rightleftharpoons}} \mathrm{PANI} + n\mathrm{Zn}^{2+} + 2n\mathrm{Cl}^{-} \qquad (1)$$

3.5. Charge/discharge test of Zn–PANI–FB

The galvanostatic charge/discharge tests of single electrodes in Zn–PANI–FB were conducted with a reference electrode (SCE). The results indicated that the IR drop was below ~0.06 V for the zinc electrode, whereas the IR drop of the flowing PANI electrode was up to ~0.31 V, which suggested that the major polarization of the battery occurred at the flowing PANI electrode.

To evaluate the performance of the present battery, the galvanostatic charge/discharge experiment of battery was carried out with PANI suspension circulated at 30 mL min^{-1} through the cathode compartment. Fig. 7 shows the capacity curves of various current densities at the potential range between 1.7 and 0.7 V. It could be seen that the discharge capacity density decreased with the increase of current density. The maximum discharge capacity density of 131.4 mAh g^{-1} was obtained at the current density of 10 mA cm^{-2}, and the discharge capacity density was near to 115.2 mAh g^{-1} at the current density of 20 mA cm^{-2}. The decrease in the capacity density of flowing PANI cathode was attributed to

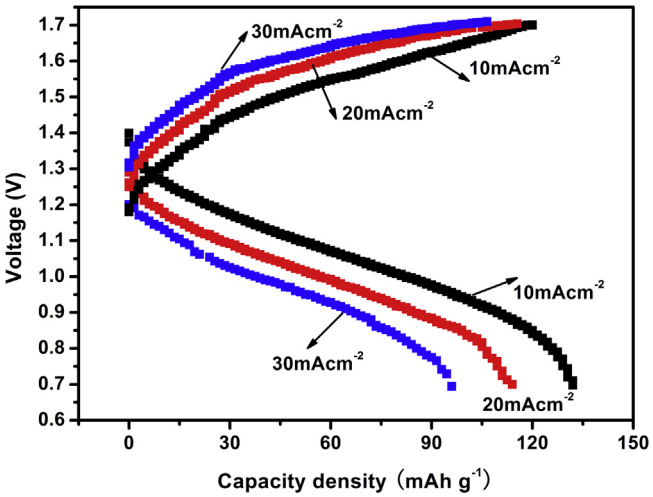

Fig. 7. Charge–discharge capacity curves at various current densities: 10, 20, 30 mA cm^{-2}, PANI suspension: 150 g L^{-1}.

the electrode polarization resulting from charge transfer resistance and diffusion overpotential at the higher current density. Additionally, the utilization ratio of PANI particles during redox process was less than 100% according to the size dependence principle of partial electrons transfer of particles [19], which was also responsible for decay of the capacity of PANI cathode. Nevertheless, the capacity density of the present flow battery was higher than that of the PANI film battery, in which only out-layer of PANI film material took apart in the charge/discharge process, whereas, a large amount of PANI material was stored in the external reservoir in the flow battery system, taking more percentage of the total weight of battery.

From Fig. 7, we could find that the coulombic efficiency of charge/discharge cycle strongly depended on the current density. The coulombic efficiency was about 97% at the current density of 20 mA cm^{-2}, while the coulombic efficiency of 10 mA cm^{-2} arrived at 118% (based on the weight of dry PANI powder). As for the coulombic efficiency exceeding 100%, it could be attributed to the oxidation of the PANI particles by the atmospheric oxygen [20,21]. When the battery worked at the lower current density, the longer time the charge/discharge cycle took, the more PANI material was oxidized by the atmospheric oxygen, so the coulombic efficiency increased with the decrease of current density. On the other hand, some PANI oligomer and part of PANI particles with diameter below 500 nm could pass through the microporous membrane to transfer anolyte compartment, which might cause the self-discharging occurrence and the decrease of coulombic efficiency. However, our experimental results showed this self-discharging was not dominated in comparison with the oxidation of PANI by the atmospheric oxygen.

The Zn–PANI–FB exhibited a significant improvement on the charge/discharge current density compared with the conventional Zn–PANI film batteries such as 0.05, 0.1 mA cm^{-2} [7], 0.25–1 mA cm^{-2} [22], 0.5, 2.5 mA cm^{-2} [5]. In this study the current density of 30 mA cm^{-2} was achieved with the coulombic efficiency of 85.9% for the small laboratory battery. The current density was at least ten times higher than that of the aforementioned semi-solid lithium rechargeable flow battery, and almost approached the level of conventional RFB (25–100 mA cm^{-2}) [23].

Fig. 8 shows the charge/discharge response during repeated cycles at the current density of 20 mA cm^{-2}. As seen from the inset, the well defined charge/discharge curves were exhibited, and the battery presented a slope discharge curve in the voltage of 1.4 V–0.8 V. A sudden drop in the cell potential at the start of discharge

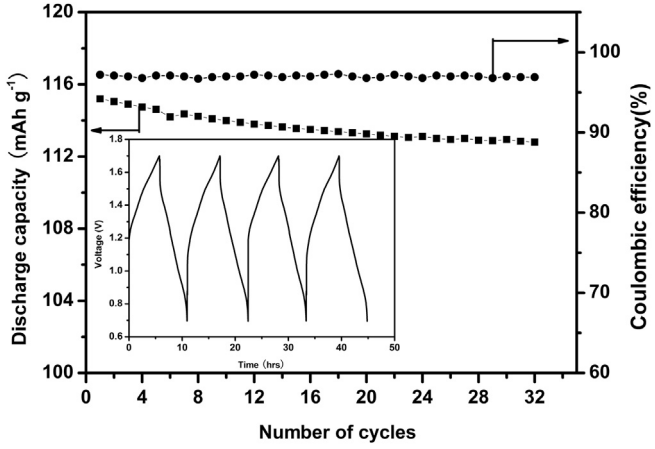

Fig. 8. Coulombic efficiency and discharge capacity vs. cycle number for Zn–PANI–FB at a constant current density of 20 mA cm^{-2}; Potential-time curve at current density of 20 mA cm^{-2} (inset). PANI suspension: 150 g L^{-1}.

was proportional to the current density, which resulted from the charge transfer resistance, and the voltage changed smoothly except in the end period of discharge. The average discharge voltage of this battery was about 1.1 V. The discharge capacity density decreased with the number of charge/discharge cycle from 115.2 mAh g^{-1} to 112.8 mAh g^{-1}, and the average of discharge capacity loss during 32 cycles was 0.07% per cycle. The decrease of discharge capacity was possibly due to the electrochemical degradation of cathode material resulting from overoxidation of PANI. The battery presented an average coulombic efficiency of 97% at the current density of 20 mA cm^{-2}, and the value of coulombic efficiency showed no significant change with the number of cycles over the experiment.

4. Conclusions

In conclusion, we have demonstrated the feasibility of Zn–PANI–FB using PANI suspension as flowing cathode and zinc as anode. Transition from solid film to a flow-through mode for cathode material enabled the battery to operate at higher current density (The discharge current density of 30 mA cm^{-2} was achieved.) and if appropriate configuration can be constructed, to achieve higher power. Based on redox potential and content of the PANI materials studied here, the PANI cathode has maximum theoretical energy density of 66.5 Wh L^{-1}, which is higher than state-of-the-art all-vanadium RFB (~40 Wh L^{-1}) [23]. The present findings could mark a new route to improve the performance of conductive polymer-based energy storage devices by employing polymer suspensions as electrode materials.

Acknowledgment

This work was supported by the Fundamental Research Funds for the Central Universities of Central South University (NO.:2013zzts016).

References

[1] S.K. Mondal, K. Barai, N. Munichandraiah, Electrochim. Acta 52 (2007) 3258–3264.
[2] Z. Mandić, M.K. Roković, T. Pokupcić, Electrochim. Acta 54 (2009) 2941–2950.
[3] L. Liu, F. Tian, M. Zhou, H. Guo, X. Wang, Electrochim. Acta 70 (2012) 360–366.
[4] B.N. Grgur, A. Žeradjanin, M.M. Gvozdenović, M.D. Maksimović, T.Lj. Trišović, B.Z. Jugović, J. Power Sources 217 (2012) 193–197.
[5] S. Li, G. Zhang, G. Jing, J. Kan, Synth. Met. 158 (2008) 242–245.
[6] J. Zhang, D. Shan, S. Mu, J. Power Sources 161 (2006) 685–691.
[7] M. Sima, T. Visan, M. Buda, J. Power Sources 56 (1995) 133–136.
[8] B.Z. Jugović, T.Lj. Trišović, J. Stevanović, M. Maksimović, B.N. Grgur, J. Power Sources 160 (2006) 1447–1450.
[9] A. Mirmohseni, M.R. Milani, V. Hassanzadeh, Polym. Int. 48 (1999) 873–878.
[10] F. Beck, P. Ruetschi, Electrochim. Acta 45 (2000) 2467–2474.
[11] M. Skyllas-Kazacos, D. Kasherman, R.R. Hong, M. Kazacos, J. Power Sources 35 (1991) 399–404.
[12] A. Price, S. Bartley, S. Male, G. Cooley, Power Eng. J. 13 (1999) 122–125.
[13] W. Wang, Z. Nie, B. Chen, F. Chen, Q. Luo, X. Wei, G. Xia, M. Skyllas-Kazacos, L. Li, Z. Yang, Adv. Energy Mater. 2 (2012) 487–493.
[14] M. Duduta, B. Ho, V.C. Wood, P. Limthongkul, V.E. Brunini, W.C. Carter, Y. Chiang, Adv. Energy Mater. 1 (2011) 511–516.
[15] K. Aoki, T. Lei, Langmuir 16 (2000) 10069–10075.
[16] Kh. Ghanbari, M.F. Mousavi, M. Shamsipur, Electrochim. Acta 52 (2006) 1514–1522.
[17] F. Rahman, M. Skyllas-Kazacos, J. Power Sources 189 (2009) 1212–1217.
[18] S. Zhu, W. Sun, Q. Wang, H. Yin, B. Wang, Chem. Ind. Eng. Prog. 26 (2007) 207–211.
[19] C. Xu, K. Aoki, Langmuir 20 (2004) 10194–10199.
[20] N. Gospodinova, V. Must, H. Kolev, J. Romanova, Synth. Met. 161 (2011) 2510–2513.
[21] A. Wu, E.C. Venancio, A.G. MacDiarmid, Synth. Met. 157 (2007) 303–310.
[22] B.Z. Jugović, T.Lj. Trišović, J.S. Stevanović, M.D. Maksimović, B.N. Grgur, Electrochim. Acta 51 (2006) 6268–6274.
[23] L. Li, S. Kim, W. Wang, M. Vijayakumar, Z. Nie, B. Chen, J. Zhang, G. Xia, J. Hu, G. Graff, J. Liu, Z. Yang, Adv. Energy Mater. 1 (2011) 394–400.